Theoretical study of the group-IV antisite acceptor defects in $CdGeAs_2$

Miguel A. Blanco,[a] Aurora Costales,[a] and Victor Luaña
Departamento de Química Física y Analítica, Facultad de Química, Universidad de Oviedo, 33006-Oviedo, Spain

Ravindra Pandey[b]
Department of Physics, Michigan Technological University. Houghton, Michigan 49931

(Received 7 July 2004; accepted 14 September 2004)

Native and impurity antisite point defects in $CdGeAs_2$ are studied here using an embedded quantum cluster model based on density functional theory. The calculated geometric relaxations and spin densities of the antisite defects considered here show a clear and distinct difference in the nature of native (i.e. $[Ge_{As}]$) and impurity (i.e. $[C_{As}]$ and $[Si_{As}]$) antisite defects in $CdGeAs_2$. For the native antisite acceptor, the hole appears to be delocalized in contrast to impurity antisites where the hole is mainly localized at the acceptor site. © *2004 American Institute of Physics*.
[DOI: 10.1063/1.1818731]

Cadmium germanium arsenide ($CdGeAs_2$) is an ideal candidate material for nonlinear optical (NLO) applications, since it has the highest NLO coefficient, 236 pm/V, known for a phase matchable compound semiconductor.[1,2] Recent successes[3] in the horizontal gradient freeze growth technique made it possible to grow large single crystals of $CdGeAs_2$ which led to renewed efforts to utilize this material for optoelectronic devices. However, a discrete absorption band near 5.5 μm is found to hinder the performance of devices. This absorption band is attributed to acceptor levels in $CdGeAs_2$.[4–7] A recent experimental study[8] further confirms the association of a paramagnetic state of the acceptor level to the absorption band at 5.5 μm. The most likely candidate for the acceptor level was suggested to be the Ge-on-As antisite (i.e. $[Ge_{As}]$) defect, though a small possibility was allowed for impurities, such as C or Si antisites.

In this work, our aim is to obtain local electronic and structural properties of native and impurity antisite defects in $CdGeAs_2$. Specifically, we will perform embedded quantum cluster calculations, based on density functional theory (DFT) to calculate the spin densities over the near neighbors for the antisite defects in the lattice. Although there exist alternative first-principle methods to compute the geometrical and electronic properties, such as the supercell or the Green's function approaches, the advantage of the present method is that it can access the local electronic properties, unlike the former, and it uses standard quantum-mechanical codes, unlike the latter.

In our embedded quantum cluster method, there are four principal components which need to be described carefully. These are: (i) The finite point-charge set that simulates the long-range electrostatic potential of the crystalline lattice, (ii) the crystal-adapted pseudopotentials (caPS) for atoms at the cluster boundary simulating the short-range Coulomb and overlap repulsions to the cluster atoms, (iii) the Gaussian basis sets with which the electron density of the cluster atoms is described, and (iv) the cluster-lattice partition, which facilitates the interfacing of the cluster with the crystalline lattice in a way which appropriately embeds the electron density of the cluster within the lattice appropriately.

In $CdGeAs_2$, tetrahedral coordination of the atoms suggests that the covalent bonding predominates, while the composition of the cation sublattice indicates a partial ionic character. Realizing this, we therefore do not consider a fully ionic model assuming Cd^{2+}, Ge^{4+}, and As^{3-} ions, rather we perform a first-principles crystalline calculation followed by an atoms in molecules (AIM)[9] analysis to evaluate the charge localized within the basin of each given atom in the lattice. The AIM calculation yields fractional charges of $+0.62$ for Cd, $+0.71$ for Ge and -0.665 for As in $CdGeAs_2$. Employing the AIM charges, we now build the point-charge set in which the calculated electrostatic potential mimics the shape and the features of the perfect lattice potential very well. It is well known that the finite point-charge set generally introduces a global shift of the electrostatic potential and its multipole derivatives at the origin. Since the As site in $CdGeAs_2$ has C_2 symmetry, a small set of ghost point charges is selected as an orthohedron parallel to the unit cell, with charges and edge ratios chosen such that the potential, and both its gradient and hessian at the As site exactly match those of the perfect lattice.

For the cluster atoms, we took the CRENBL effective core potential (ECP) plus double-zeta valence Gaussian basis set,[10] and reoptimized the largest exponents of the basis sets within the $CdGeAs_2$ lattice.[11] On the other hand, the cluster boundary atoms are represented by caPS that essentially mimic the quantum embedding potential of an ion.[12] The caPS for the host atoms were derived at the prefect crystal geometry of $CdGeAs_2$. We have used the GAUSSIAN98 program[13] to perform DFT calculations employing Becke[14] and Perdew–Wang[15] density functional forms.

Since the chalcopyrite $CdGeAs_2$ is very close to the ideal B3 structure, we will simplify the description by sorting the atoms in the lattice in B3-like connectivity shells around the central defect site. Our best cluster model (Fig. 1) is made up of the defect center (As for the nominal cluster, but C, Si, or Ge for the antisite cases), first- (2Ge+2Cd), second- (12 As), and third-neighbor (12Ge+12Cd) shells in terms of connectivity (for example, the third shell is defined as those atoms

[a]Temporary address: Department of Physics, Michigan Technological University, Houghton, MI 49931.
[b]Author to whom correspondence should be addressed, electronic mail: pandey@mtu.edu

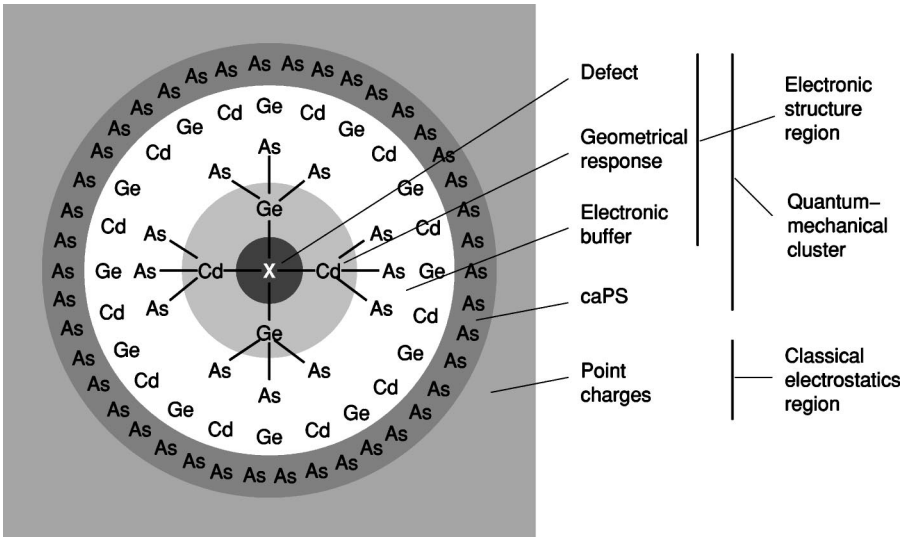

FIG. 1. Schematic representation of the cluster model.

connected to the second shell which are not in the first shell, and is composed in fact by two different distance shells, third and fifth, even in the symmetric B3 lattice). The next connectivity shell (42 As, three B3 shells in total) is substituted by caPS and no basis functions are centered on it. Finally, the classical embedding region consists of ten shells of point charges located at perfect lattice positions, plus the small group of ghost charges described before. Overall, the nominal cluster includes 83 atoms with 660 electrons described by 834 basis functions, 878 core electrons described by ECPs (in 41 atoms), 1414 electrons described by caPS (in 42 atoms), and 260 point charges representing the electrostatic potential.

The defect center and its first neighbor shell are the only atoms allowed to move in the geometrical optimization. The second- and third-neighbor shells, forming the cluster boundary, are kept at the geometry they would have in the unrelaxed lattice. Since they are part of the cluster, the electron density over them will respond to the geometrical changes in the cluster, accommodating these changes to the lattice geometry, thus acting as a buffer between the fully (i.e., electronically and geometrically) relaxed inner cluster, and the fully frozen external lattice, improving the description of the defect region.

We first consider equilibration in our model between the perfect-crystal arsenic-centered embedded cluster (i.e. [As] $[Ge_2+Cd_2][As_{12}][Ge_{12}+Cd_{12}]$) and the embedding lattice. In this self-embedding model, R_{Ge-As} is about 1.4% larger and R_{Cd-As} is 1.7% smaller than the corresponding experimental values[16] (Table I) indicating that, at least with respect to cluster-embedding compatibility, our model is quite reasonable.

It should be kept in mind that the As site has C_2 symmetry in the lattice, allowing the central atom to move during the geometry optimization of the embedded quantum cluster. In all cases, we have found the central As atom to be displaced along the C_2 (x) axis in the direction of the Cd atom. This indicates an error in the computed electric field over the asymmetric As central atom, due to the approximate nature of the classical region. However, this error is small and systematic, in the sense that all of the perfect and defect-containing clusters show it.

To account for the small systematic embedding errors in the geometrical parameters, we can use a self-embedding correction.[17] Accordingly, we will calculate the difference between the corresponding self-embedding cluster and defect cluster to model the deviation of a geometrical parameter in going from the perfect lattice to the defective lattice. Any systematic deviation in the embedding model is assumed to present and equivalent in both cluster calculations, and thus the difference gives the deviation introduced by the defect only.

The ΔR_{Ge-As} (ΔR_{Cd-As}) values are $-0.487(-0.334)$, $-0.069(-0.086)$, and $-0.033(-0.051)$ Å for $[C_{As}]$, $[Si_{As}]$, and $[Ge_{As}]$ antisite defects, respectively, after applying the self-embedding correction. In all cases, near-neighbor Ge/Cd atoms show inward relaxations whose magnitude decreases in going from C to Si to Ge in the lattice. The relatively large inward relaxation of near neighbors for $[C_{As}]$ is probably due to its electronegativity, larger than that of As, allowing for a more localized electron density and polar bonding, and also because of its small size, which leads to a non-negligible shrinking of the first coordination sphere and larger geometrical effects. Regarding the corrected displacements along x the direction, they are about 0.2 Å for C, near 0.07 Å for Si, and negligible for Ge antisites, indicating again a larger deformation and local effects for $[C_{As}]$.

In the unrestricted DFT calculations, spin-up and spin-down electrons are treated separately, so that if there is an unpaired electron, as in the clusters containing antisite defects, cluster atoms will be spin polarized. The relevant experimental evidence is in the form of spin densities derived from the ENDOR data. Since our self-embedding cluster is

TABLE I. Bond distances (Å) and angles (degree) in the optimized configurations of perfect lattice and defect clusters.

	R_{Ge-As}	R_{Cd-As}	$\alpha_{Ge-As-Ge}$	$\alpha_{Cd-As-Cd}$
$CdGeAs_2$ lattice[a]				
	2.430	2.632	101.91	114.56
Perfect-lattice cluster				
$[As_{As}]$	2.465	2.586	102.69	112.60
Anti-site defect clusters				
$[C_{As}]$	1.978	2.252	102.11	112.61
$[Si_{As}]$	2.381	2.500	104.86	110.44
$[Ge_{As}]$	2.432	2.535	101.35	114.16

[a]See Ref. 16.

TABLE II. The calculated spin density (in MHz: Isotropic Fermi contact coupling term) in antisite defect clusters.

	Defect center	First neighbors	Second neighbors
$[C_{As}]$	−12.93	0.00	0.00
$[Si_{As}]$	6.00	0.00	0.00
$[Ge_{As}]$	0.00	0.00	−0.01

diamagnetic, there is no need for a correction in spin density, and calculations can proceed as the case with isolated molecules.

The spin polarization effects due to the paramagnetic antisite defects in $CdGeAs_2$ at nuclear sites are collected in Table II. The spin density at the defect site is appreciable for $[C_{As}]$ and $[Si_{As}]$, but it is almost negligible for $[Ge_{As}]$. On the other hand, there is a small but significant polarization at the second-neighbor 12 As sites for $[Ge_{As}]$. The first and second neighbors of the central $[C_{As}]$ and $[Si_{As}]$ atoms do not show any spin polarization due to impurity antisites in the lattice.

For paramagnetic acceptor centers in a given lattice, the degree of localization of the trapped hole at and around the acceptor sites can be obtained from the magnitude of spin densities. The neutral defects considered here are acceptors in $CdGeAs_2$, and Table II shows their different natures with respect to spin localization. For $[C_{As}]$ and $[Si_{As}]$, the hole is mainly localized on the antisite defect site, while for $[Ge_{As}]$ the hole is delocalized over the central antisite and second As neighbors. This difference in the degree of localization can easily be attributed to the differences in the chemical nature of C, Si, and Ge atoms, as dicussed earlier.

Analysis of the electron paramagnetic resonance hyperfine interactions in $CdGeAs_2$ has identified the paramagnetic acceptor center associated with the 5.5 μm absoption band in $CdGeAs_2$ to be located on the As lattice site. Assuming equal hyperfine interactions with neighboring Cd and Ge nuclei, the EPR simulation program reproduced the experimental data reasonable well,[8] hinting at the delocalization of the hole. It was further suggested that the primary candidate for this center is $[Ge_{As}]$, though the possibility of $[C_{As}]$ or $[Si_{As}]$ can not be ruled out.[8] The present study clearly shows a distinct difference in the nature of the native (i.e. $[Ge_{As}]$) antisite acceptor or impurity ($[C_{As}]$ or $[Si_{As}]$) antisite acceptors, since the native case shows spin delocalization while the impurity case does not.

In order to estimate the location of the acceptor level in the band gap, we have computed the ionization potentials (IP) of the different antisite defects as well as of the self-embedding cluster. However, these values carry a large correlation error, since the IPs involve substracting energies for systems with different numbers of electrons; for example, the band gap is estimated to be 1.58 eV, much higher than the experimental value. If we include a semiempirical correlation correction to the IPs (i.e., the known correlation error for the calculations of the free atoms), the Ge antisite appears within the gap, with an IP of 0.36 eV with respect to the conduction band, while both and C Si appear within the conduction band, 0.09 and 0.71 eV, respectively, above its lower limit. The corrected gap value is 1.10 eV, still larger than the experimental value of 0.69 eV. If we further scale the energies to reproduce the experimental band gap, the resultant Ge antisite level comes out to be 0.226 eV or 5.49 μm, strongly suggesting that the Ge antisite is the origin of the observed 5.5 μm absorption band in $CdGeAs_2$, though a detailed ENDOR study is warranted to ascertain this conclusion.

In summary, we have developed an embedded quantum cluster model for point defects in $CdGeAs_2$ using state-of-the-art techniques. The calculated geometric relaxations and spin densities of the antisite defects considered here show a clear and distinct difference in the nature of native and impurity antisite defects in $CdGeAs_2$. The calculated results point to the native $[Ge_{As}]$ antisite defect to be the primary candidate for the acceptor center associated with the 5.5 μm absoption band in $CdGeAs_2$.

This work was done at Michigan Tech University under support by the Air Force Office of Scientific Research Multi-University Research Initiative (MURI) program through Grant No. F49620-01-1-0428. The spanish team acknowledges the support of the Ministerio de Ciencia y Tecnología under Grant. BQU2003-06553, and ACC's Ramón y Cajal position.

[1] R. L. Byer, H. Kildal, and R. S. Feigelson, Appl. Phys. Lett. **19**, 237 (1971).
[2] M. C. Ohmer and R. Pandey, Mater. Res. Bull. **23**, 16 (1998).
[3] P. G. Schunemann and T. M. Pollak, J. Cryst. Growth **174**, 272 (1997).
[4] B. K. Mamedov and E. O. Osmanov, Sov. Phys. Semicond. **5**, 1120 (1972).
[5] V. N. Brudnyi, M. A. Krivov, A. I. Potapov, IO. K. Polushina, V. D. Prochukhan, and Y. V. Run, Phys. Status Solidi A **49**, 761 (1978).
[6] I. Zwieback, D. Perlov, J. P. Maffetone, and W. Ruderman, Appl. Phys. Lett. **73**, 2185, (1998).
[7] L. E. Halliburton, G. J. Edwards, P. G. Schunemann, and T. M. Pollak, J. Appl. Phys. **77**, 435 (1994).
[8] L. Bai, N. Garces, N. Yang, P. G. Schunemann, D. Setzler, T. M. Pollak, L. E. Halliburton, and N. C. Giles, Mater. Res. Soc. Symp. Proc. **744**, 537 (2003).
[9] R. F. W. Bader, *Atoms in Molecules* (Oxford University Press, Oxford 1980).
[10] M. M. Hurley, L. Fernández Pacios, P. A. Christiansen, R. B. Ross, and W. C. Ermler, J. Chem. Phys. **84**, 6840 (1986); L. A. LaJohn, P. A. Christiansen, R. B. Ross, T. Atashroo, and W. C. Ermler, *ibid.* **87**, 2812 (1987).
[11] The details of the the basis sets, ECPs, and caPS, can be obtained from the authors.
[12] V. Luaña, J. M. Recio, A. Martín Pendás, M. A. Blanco, L. Pueyo, and R. Pandey, Phys. Rev. B **64**, 104102 (2001).
[13] *Gaussian 98* (Gaussian, Inc., Pittsburgh, PA, 1998).
[14] A. D. Becke, Phys. Rev. A **38**, 3098 (1988).
[15] J. P. Perdew and Y. Wang, Phys. Rev. B **45**, 13244 (1992).
[16] S. C. Abrahams and J. L. Bernstein, J. Chem. Phys. **61**, 1140 (1974).
[17] V. Luaña and M. Flórez, J. Chem. Phys. **97**, 1140 (1992).